Electronic Supplementary Material (ESI) for Inorganic Chemistry Frontiers.

Electronic Supplementary Information

Cation Reduction and Comproportionation as Novel Strategies to Produce High Voltage, Halide Free, Carborane Based Electrolytes for Rechargeable Mg Batteries

Scott G. McArthur, Linxiao Geng, Juchen Guo,* Vincent Lavallo*

Table of Contents

General Considerations

Unless otherwise stated all manipulations were carried out using standard Schlenk or glovebox techniques (O_2, H_2O < 1ppm) under a dinitrogen or argon atmosphere. Solvents were dried on K, Na or CaH_2, and distilled under argon before use. Ph_2Mg was prepared according to literature methods.[1] Reagents were purchased from commercial vendors and used without further purification. NMR spectra were recorded on Bruker Avance 300 MHz, Varian Inova 300 MHz, Varian Inova 400 MHz, or Varian Inova 500 MHz spectrometers. NMR chemical shifts are reported in parts per million (ppm). ^{1}H NMR and ^{13}C NMR chemical shifts were referenced to residual solvent. ^{11}B NMR chemical shifts were externally referenced to BF_3OEt_2.

Synthesis of 1[Mg^{2+}]

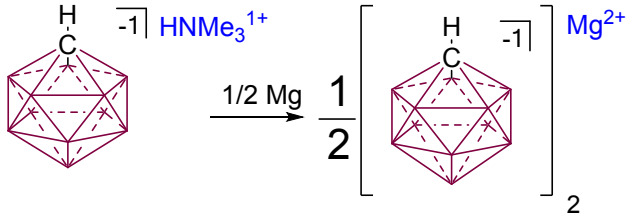

1[$HNMe_3^{1+}$] **1[Mg^{2+}]**

1[$HNMe_3^{1+}$] (2.0 g, 10.3 mmol) was added to a suspension of Mg powder (4.0 g, 165 mmol) in a minimal amount of THF (5mL) and the resulting suspension was stirred for 1 hr. After 1 hr, additional THF (30mL) was added and the suspension was left to stir for 24 hours. The THF solution was then filtered through a medium porosity fritted funnel. The collected precipitate of white powder and excess magnesium was washed with DME, dissolving the white powder of the collected precipitate. Unreacted magnesium powder was collected and reused. The DME solvent was removed under high vacuum, resulting in compound **1[Mg^{2+}]** as a white powder in 91% yield (5.44 g 9.37 mmol) (**Note:** Mg^{2+} counter cations contain 3 coordinated DME molecules). Once dried, compound **1[Mg^{2+}]** is only soluble in DME at cold temperatures -30°C (**Note:** Mg^{2+} counter cation is coordinated to three DME molecules). The reaction progress is monitored using ^{1}H NMR by the loss of trimethyl ammonium counter cation peak at δ = 3.19 ppm in acetone-d_6. ^{1}H NMR (300 MHz, acetone-d_6, 25°C): δ = 3.46 (s, 4H), 3.28 (s, 6H), 2.50-0.75 (bm, 11 H, B-*H*) ppm; ^{1}H{^{11}B} NMR (300 MHz, acetone-d_6, 25 °C): δ = 3.46 (s, 4H), 3.28 (s, 6H), 2.22 (s, 1H, B-*H*); ^{11}B {^{1}H} NMR (96 MHz, acetone-d_6, 25 °C): δ = -3.2, -9.6, -12.6 ppm.

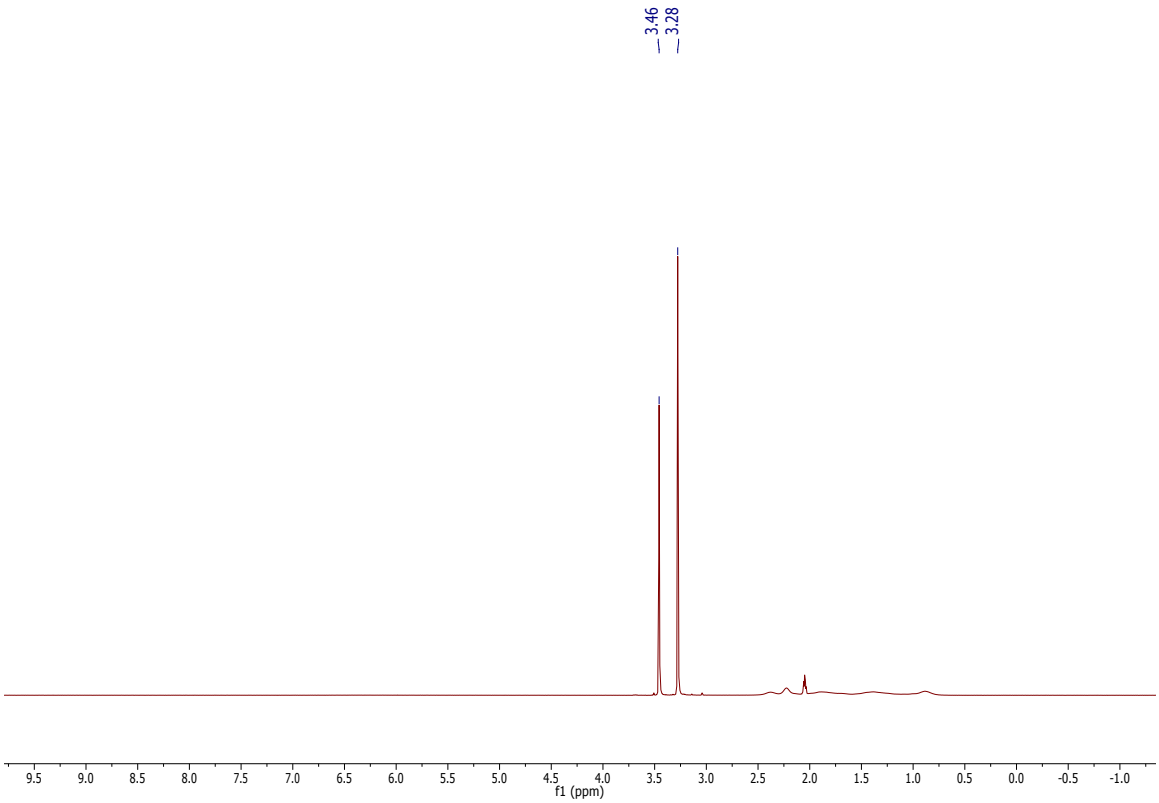

Figure S1. ^{1}H NMR of **1[Mg^{2+}]** in acetone-d_6 (**Note:** peaks at 3.45 and 3.28 ppm are DME).

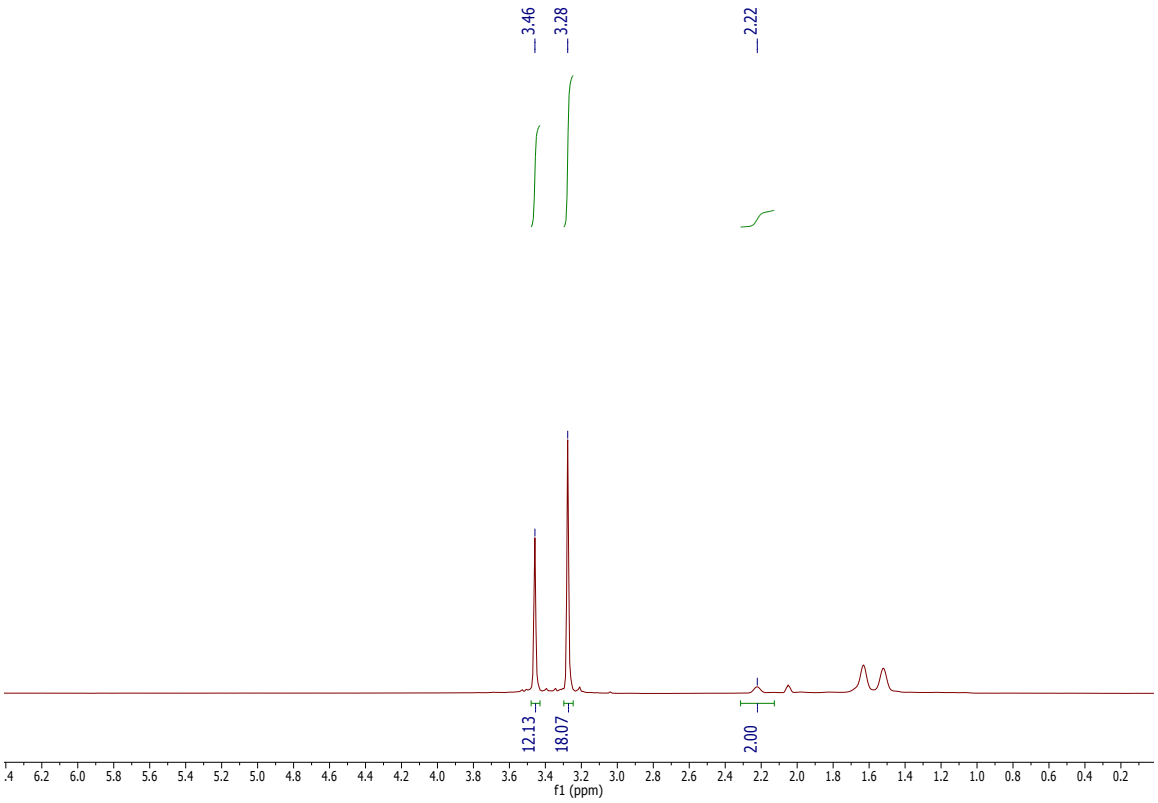

Figure S2. $^{1}H\{^{11}B\}$ NMR of **1[Mg^{2+}]** in acetone-d_6. Integration of antipodal B-H of the carborane (2.22 ppm) and intergration of DME signals (3.46 and 3.28 ppm) is used to determine the number of coordinated DME molecules.

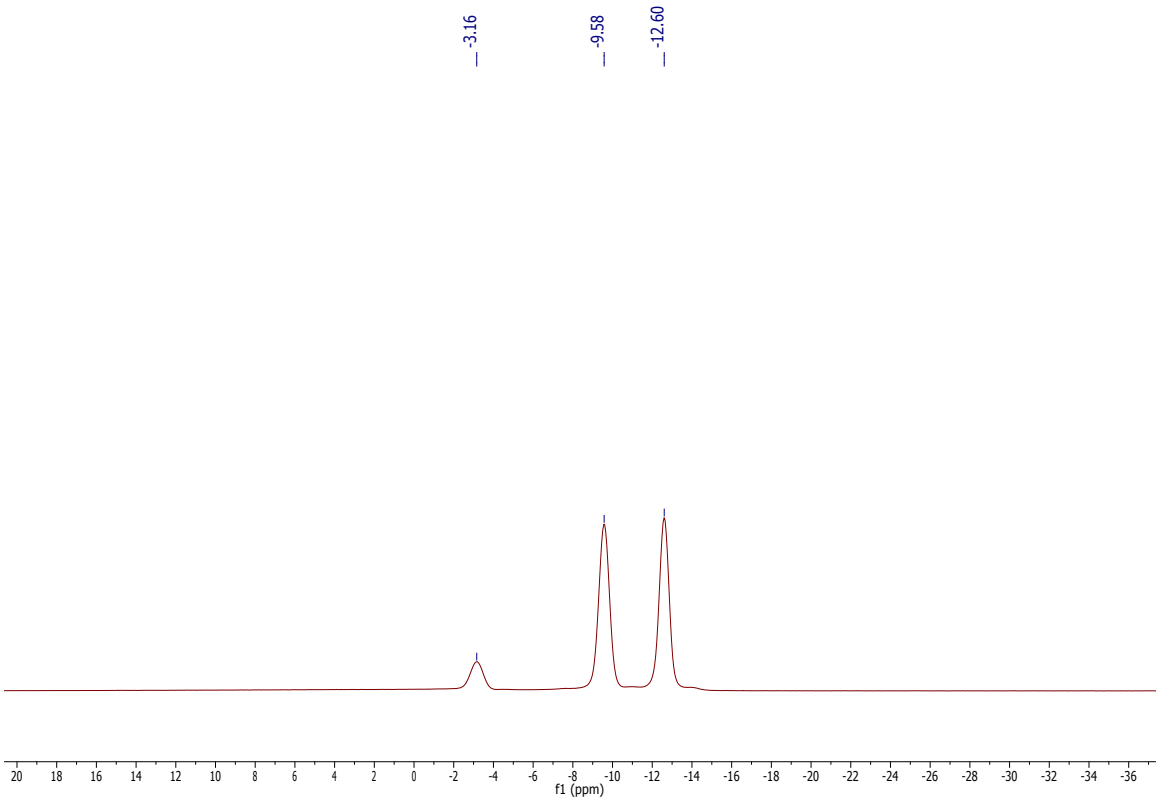

Figure S3. $^{11}B\{^{1}H\}$ NMR of compound **1[Mg^{2+}]** in acetone-d_6.

<u>Synthesis of Ph_2Mg</u>

Ph_2Mg was synthesized according to literature[1] and recrystallized in DME at -30°C (**Note:** Ph_2Mg has 1/2 coordinated DME molecule). ^{1}H NMR (400 MHz, THF-d_8): δ = 7.94 (d, $^{3}J(H,H)$= 6.4 Hz, 2H), δ = 6.87 (dd, $^{3}J(H,H)$= 7.6, 7.2 Hz, 2H), δ = 6.75 (t, $^{3}J(H,H)$= 7. Hz, 1H); $^{13}C\{^{1}H\}$ NMR (300 MHz, DME): δ = 180.4 (ipso *C*H), δ = 143.2 δ = 125.2 δ = 123.1 ppm.

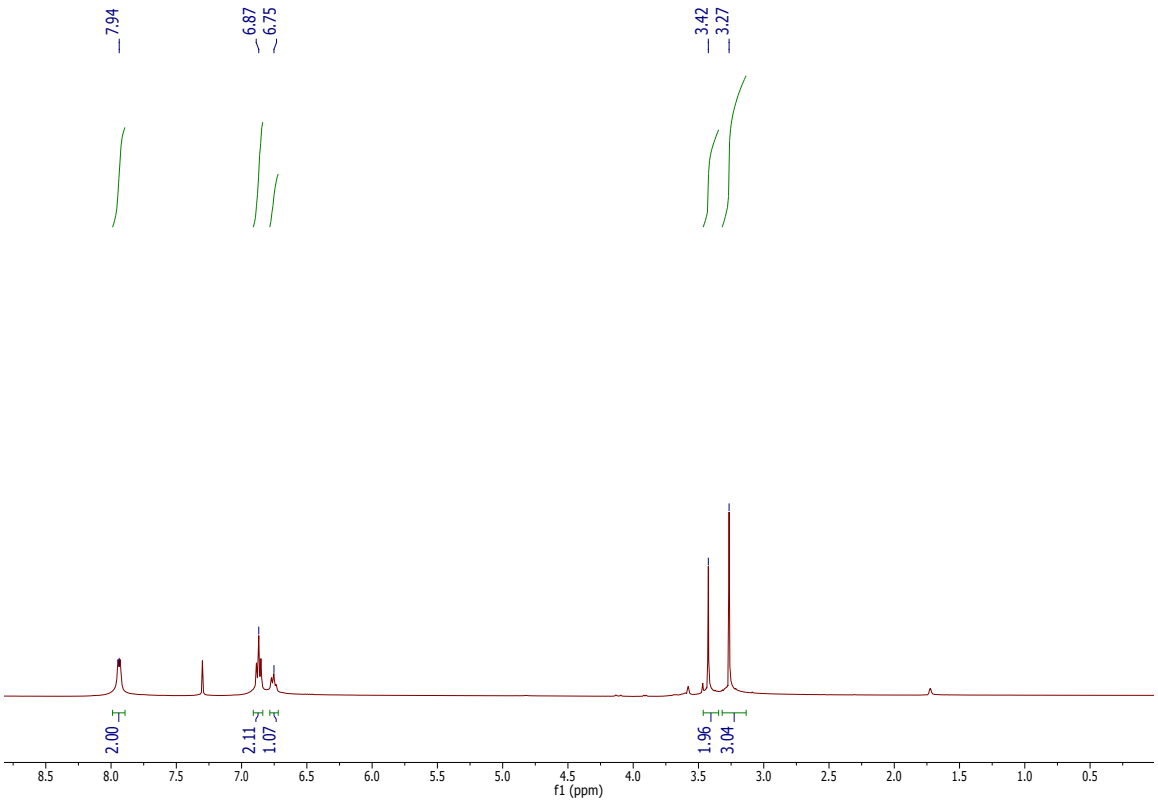

Figure S4. ^{1}H NMR of Ph_2Mg in THF-d_8 (**Note**: Minute amounts of adventitious water in the NMR solvent leads to partial protonolysis of the reactive Mg-Ph bond, which explains the trace of protio benzene in the NMR spectra at 7.30 ppm. Coordinated DME 3.43 ppm, 3.27 ppm).

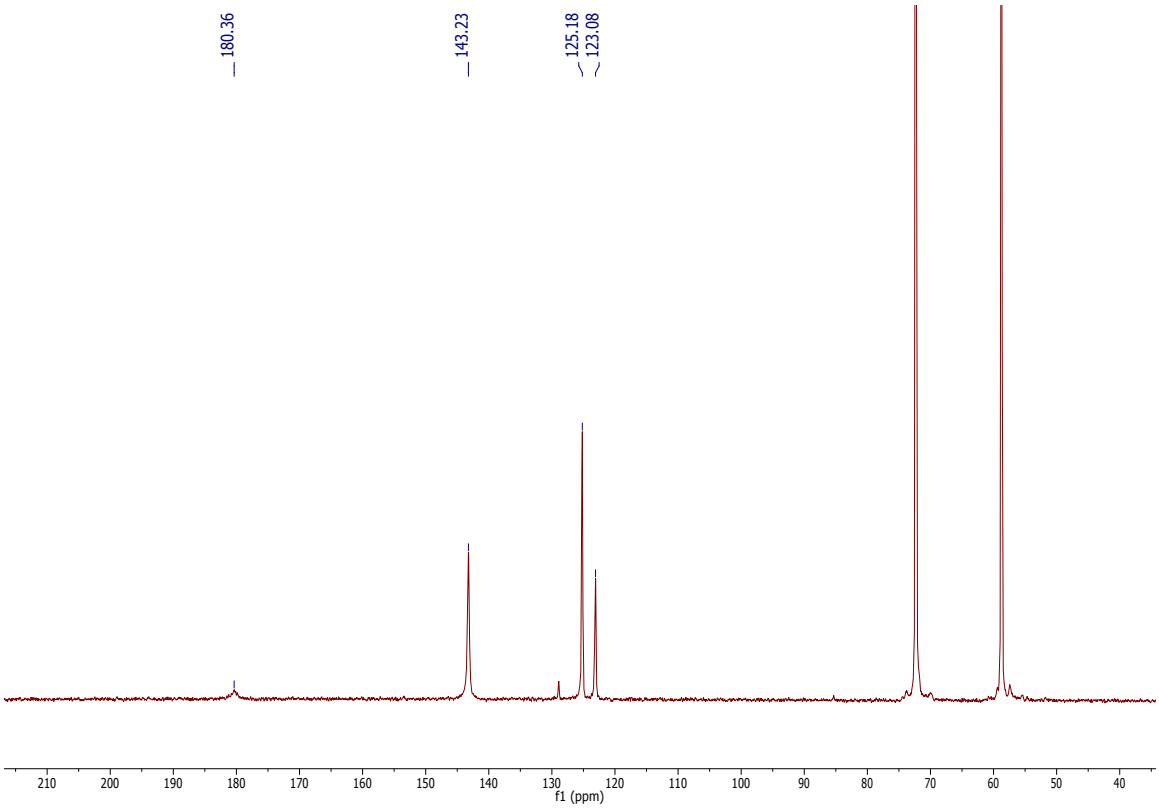

Figure S5. $^{13}C\{^{1}H\}$ NMR of Ph_2Mg in DME (**Note:** Minute amounts of adventitious water in the NMR solvent leads to partial protonolysis of the reactive Mg-Ph bond, which explains the trace of protio benzene in the NMR spectra at 128.9 ppm)

Synthesis of 1[MgPh^{1+}]

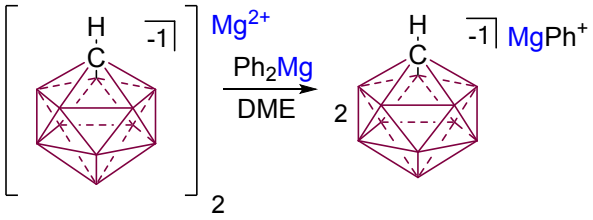

1[Mg^{2+}] **1[MgPh^{1+}]**

Crystalline Ph_2Mg (580 mg, 2.15 mmol) was dissolved in DME and added to a stirring suspension of **1[Mg^{2+}]** (1.25 g, 2.15 mmol) in 10mL DME. Addition of Ph_2Mg instantly solubilizes the suspension. DME is removed under high vacuum, affording **1[MgPh^{1+}]** in 92% yield (1.68g, 3.9 mmol) (**Note:** MgPh cation contains 2 DME molecules coordinated). Crystal suitable for single crystal diffraction was obtained by crystallization in toluene at -35°C. ^{1}H NMR (400 MHz, THF-d_8, 25°C): δ = 7.52 (d, $^{3}J(H,H)$ = 6.40 Hz, 2 H), 6.95 (dd, $^{3}J(H,H)$ = 6.80, 8.61 Hz, 2 H), 6.83 (t, $^{3}J(H,H)$ = 6.80 Hz, 1 H), 2.2-0.85 (bm, 11H, B-*H*) ppm; ^{13}C{^{1}H} NMR (300 MHz, THF-d_8, 25°C): δ = 168.9 (ipso *C*H), 140.0, 124.9, 123.0 ppm; ^{11}B{^{1}H} NMR (96 MHz, DME, 25 °C): δ = -4.2, -10.6, -13.7 ppm.

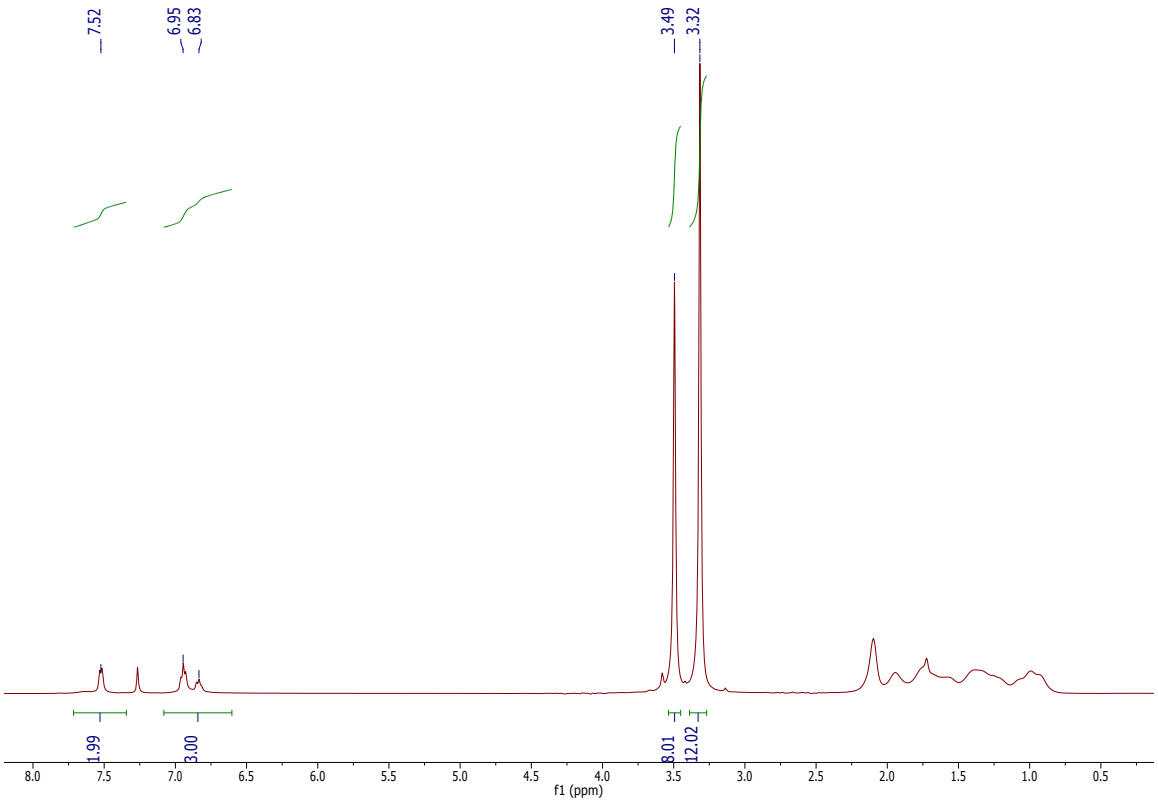

Figure S6. ^{1}H NMR of **1**[MgPh^{1+}] in THF-d_8 (**Note:** Minute amounts of adventitious water in the NMR solvent leads to partial protonolysis of the reactive Mg-Ph bond, which explains the trace of protio benzene in the NMR spectra at 7.26 ppm. Coordinated DME 3.50 ppm, 3.32 ppm).

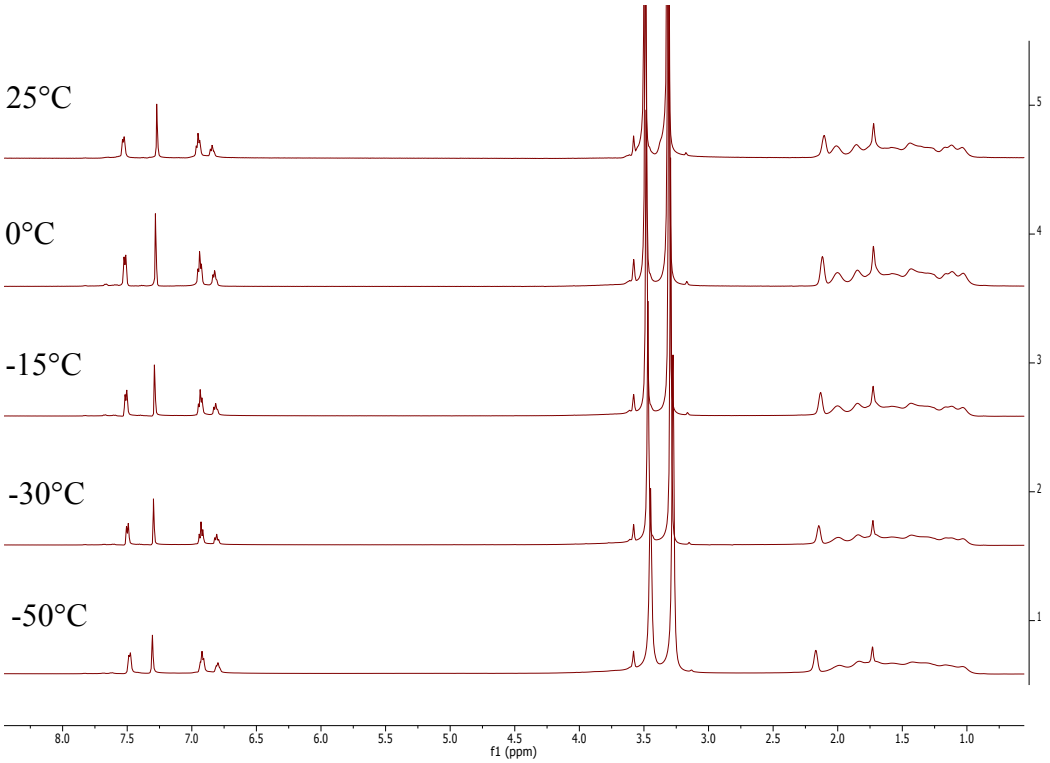

Figure S7. Variable temperature ^{1}H NMR of **1[MgPh^{1+}]** in THF-d_8 (**Note**: Minute amounts of adventitious water in the NMR solvent leads to partial protonolysis of the reactive Mg-Ph bond, which explains the trace of protio benzene in the NMR spectra at 7.26 ppm. Coordinated DME 3.50 ppm, 3.32 ppm).

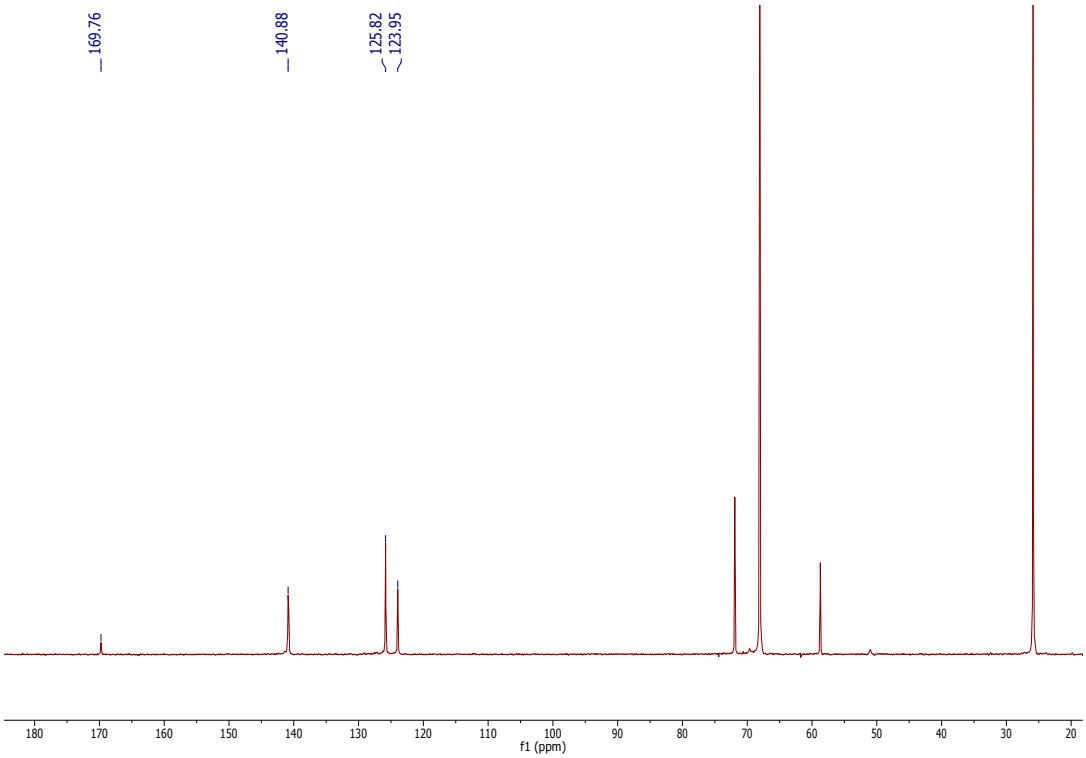

Figure S8. ^{13}C NMR **1**[$MgPh^{1+}$] in THF-d_8 (**Note**: Carbon of carborane is at 51.0 ppm).

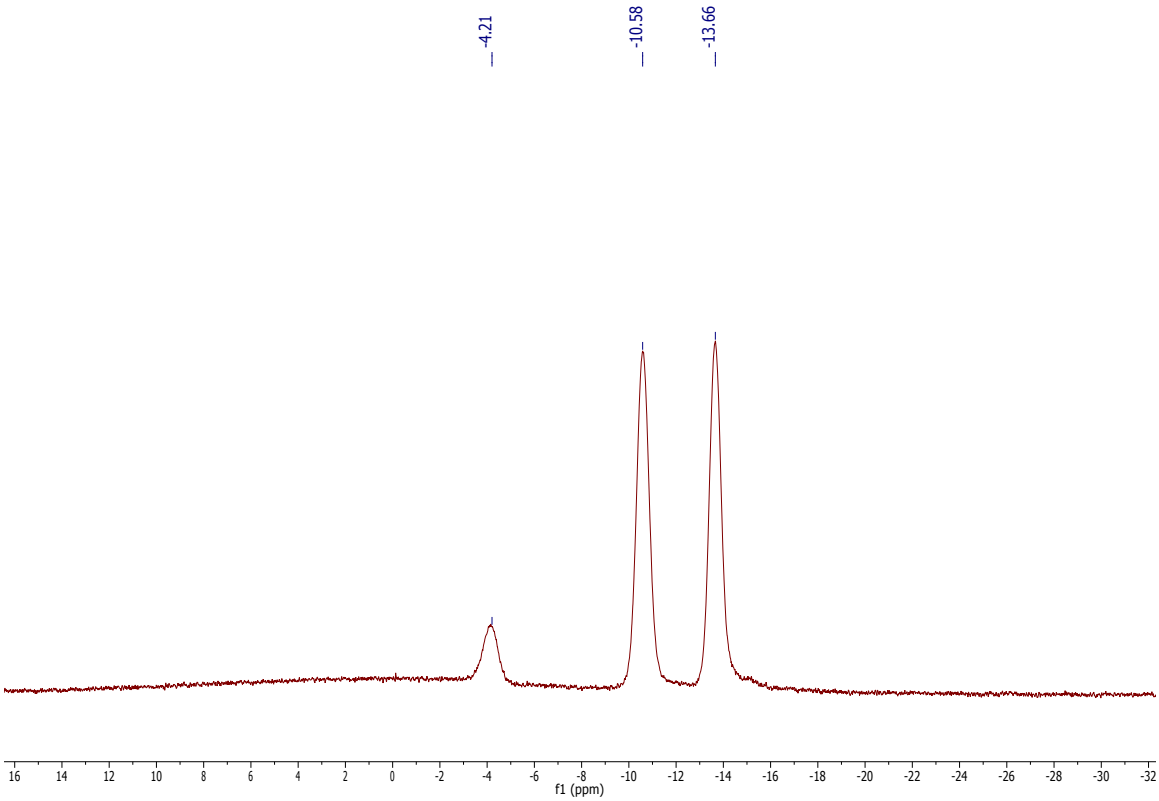

Figure S9. $^{11}B\{^{1}H\}$ NMR of **1**[$MgPh^{1+}$] in DME.

X-Ray Structure Determination

A colorless prism fragment (0.567 x 0.323 x 0.241 mm^3) was used for the single crystal x-ray diffraction study of $[[C_4H_{10}O_2]_2[C_4H_8O][C_6H_5]Mg]^+[CH_{12}B_{11}]^-.[C_7H_8]_2$ (sample vL149SM_0m-5). The crystal was coated with paratone oil and mounted on to a cryo-loop glass fiber. X-ray intensity data were collected at 100(2) K on a Bruker APEX2[2] platform-CCD x-ray diffractometer system (fine focus Mo-radiation, λ = 0.71073 Å, 50KV/30mA power). The CCD detector was placed at a distance of 5.0600 cm from the crystal.

A total of 4800 frames were collected for a sphere of reflections (with scan width of 0.3° in ω, starting ω and 2θ angles of –30°, and ϕ angles of 0°, 90°, 120°, 180°, 240° and 270° for every 600 frames, and 1200 frames with ϕ-scan from 0-360°, 60 sec/frame exposure time). The Bruker Cell_Now program[3] was used to obtain the two different orientation matrices of the rotational twin components (Twin law is 180° rotation about the 1 0 1 real axis). These matrices were imported into the APEX2 program for Bravais lattice determination and initial unit cell refinement. The frames were integrated using the Bruker SAINT software package[4] and using a narrow-frame integration algorithm. Based on a monoclinic crystal system, the integrated frames yielded a total of 4946 unique independent reflections [maximum 2θ = 43.932° (0.95 Å resolution), data completeness = 100%] and 4557 (92.1%) reflections were greater than 2σ(I). The unit cell parameters were, **a** = 16.659(3) Å, **b** = 13.261(3) Å, **c** = 18.213(4) Å, β = 97.572(3)°, V = 3988.1(14) $Å^3$, Z = 4, calculated density D_c = 1.134 g/cm^3. Absorption corrections were applied (absorption coefficient μ = 0.082 mm^{-1}; min/max transmission = 0.955/0.981) to the raw intensity data using the Bruker TWINABS program[5].

The Bruker SHELXTL software package[6] was used for phase determination and structure refinement. Using the first twin domain HKL 4 intensity data, the distribution of intensities and systematic absent reflections indicated one possible space group, P2(1)/n. The space group P2(1)/n (#14) was later determined to be correct. Direct methods of phase determination followed by two Fourier cycles of refinement led to an electron density map from which most of the non-hydrogen atoms were identified in the asymmetry unit of the unit cell. With subsequent isotropic refinement, all of the non-hydrogen atoms were identified. The combined (major and minor components) HKLF 5 intensity dataset was used in the final structure refinement. There was one cation of $[[C_4H_{10}O_2]_2[C_4H_8O][C_6H_5]Mg]^+$, one anion of $[CH_{12}B_{11}]^-$, and two toluene molecules present in the asymmetry unit of the unit cell. The rotational twin law was 180^o rotation about the 1 0 1 real axis. The major/minor twin component ratio was 51%/49%. The alert levels A and B are due to the poor crystal quality with low resolution data. Attempts to model the possible toluene, cation and anion disorder failed because of poor quality data with low resolution.

Atomic coordinates, isotropic and anisotropic displacement parameters of all the non-hydrogen atoms were refined by means of a full matrix least-squares procedure on F^2. The H-atoms were included in the refinement in calculated positions riding on the atoms to which they were attached. The refinement converged at R1 = 0.0985, wR2 = 0.2405, with intensity, $I>2\sigma(I)$. The largest peak/hole in the final difference map was 0.438/-0.381 e/$Å^3$.

Table 1. Crystal data and structure refinement for vL149SM_0m-5.

Identification code	vL149SM_0m-5	
Empirical formula	C33 H61 B11 Mg O5	
Formula weight	681.03	
Temperature	100(2) K	
Wavelength	0.71073 Å	
Crystal system	Monoclinic	
Space group	P 21/n (#14)	
Unit cell dimensions	a = 16.659(3) Å	α = 90°.
	b = 13.261(3) Å	β = 97.572(3)°.
	c = 18.213(4) Å	γ = 90°.
Volume	3988.1(14) $Å^3$	
Z	4	
Density (calculated)	1.134 Mg/m^3	
Absorption coefficient	0.082 mm^{-1}	
F(000)	1464	
Crystal size	0.567 x 0.323 x 0.241 mm^3	
Theta range for data collection	1.778 to 21.966°.	
Index ranges	-17<=h<=17, 0<=k<=13, 0<=l<=19	
Reflections collected	15800	
Independent reflections	4946 [R(int) = 0.0613]	
Completeness to theta = 25.242°	100.0 %	
Absorption correction	Semi-empirical from equivalents	
Refinement method	Full-matrix least-squares on F^2	
Data / restraints / parameters	4946 / 30 / 458	
Goodness-of-fit on F^2	1.159	
Final R indices [I>2sigma(I)]	R1 = 0.0985, wR2 = 0.2405	
R indices (all data)	R1 = 0.1065, wR2 = 0.2464	
Extinction coefficient	n/a	
Largest diff. peak and hole	0.438 and -0.381 $e.Å^{-3}$	

Synthesis of Mo_6S_8

All reagents were purchased from commercial vendors without further purification. In a typical synthesis of Mo_6S_8, stoichiometric amounts of anhydrous copper(II) chloride ($CuCl_2$, 0.3442 g, 2.56 mmol, Sigma Aldrich 99.995%) and ammonium tetrathiomolybdate ($(NH_4)_2MoS_4$, 2.000 g, 7.68 mmol; Fisher Scientific 99.99%) were dissolved in 65 mL N,N-Dimethylformamide (DMF, Sigma Aldrich 99.8%) and the mixture was stirred for 30 min at room temperature. The resultant solution was then heated at 90 °C for 6 hours under continuous argon bubbling. After the reaction was completed, the solution was filtered, and then 325 mL THF (1:5 by volume) was added immediately to the filtrate to initiate precipitation. The precipitate was collected by centrifuge, washed with THF and dried in the vacuum oven at 150 °C overnight. The dried solid agglomerate was then ground and heated in a tube furnace at 1000 °C for 7 hour under reducing environment (95 vol.% argon and 5 vol.% H_2) to yield Chevrel phase $Cu_2Mo_6S_8$. The obtained $Cu_2Mo_6S_8$ was then added into 20 mL 6M HCl solution. Oxygen was bubbled into the solution for 8 hours while stirring to leach out Cu to yield Mo_6S_8. After the reaction, the obtained Mo_6S_8 was centrifuged, washed with adequate amount of deionized water, and dried in vacuum oven at 50 °C overnight.

Electrochemical Analysis

The cyclic voltammetry (CV) of Mg deposition-dissolution and the galvanostatic Mg deposition were performed in three-electrode cells with a Gamry potentiostat/galvanostat/ZRA (Interface 3000) using Pt (GC, Ti, SS, Ni) working electrode and two Mg strips (Alfa Aesar 99.9%) as the counter and the reference electrodes, respectively. A constant current density of 0.5 mA cm^{-2} was applied on Pt substrate for 8 hours in electrochemical Mg deposition experiment.

The conductivity of the 1[$MgPh^{1+}$] electrolyte was obtained from the resistance measurement in a cell with two parallel Pt electrodes. The cell constant was obtained through calibration using standard aqueous KCl solutions. The resistance was measured with a Gamry potentiostat/galvanostat/ZRA (Interface 1000).

For coin cells assembly, Mg foil with 0.25 mm thickness (Alfa Aesar 99.9%) was used as the anode. Cathode was fabricated by coating Mo_6S_8 slurry onto carbon paper current collector. The slurry was made by mixing 80 wt.% Mo_6S_8, 10 wt.% carbon black, and 10 wt.% polyvinylidene fluoride in N-Methyl-2-pyrrolidone via a mechanical mixer for 5 min in an argon-filled glovebox. CR2032 coin cells were assembled in the argon-filled glovebox. The galvanostatic charge-discharge experiments of the coin cell batteries were performed on an Arbin battery test station, and the CV analysis of the Mg-Mo_6S_8 coin cells was conducted on a Gamry Interface 1000 with a scan rate of 0.1 mV s^{-1}.

Galvanostatic cycling method[7] was used for the average Mg deposition/stripping coulombic efficiency measurement on Ti, Ni, and SS working electrodes. Excess of Mg was first galvanostatically deposited on the metal electrodes with a 1 C cm^{-2} capacity (1 mA cm^{-2} for 1000 seconds), which was followed by galvanostatic cycling with a 0.25 C

cm^{-2} capacity (1 mA cm^{-2} for 250 seconds). The average coulombic efficiency (ACE) was determined by the number of cycles required to completely consume the excess Mg, using the following formula: $ACE=100\times NQ_{cy}/(NQ_{cy}+Q_{ex})$ (N is the number of cycles, Q_{cy}=0.25 C cm^{-2}, and Q_{ex}=1 C cm^{-2}). This determination of ACE of Mg deposition/stripping is more realistic to reflect the practical Mg battery design with excess of Mg at the anode.

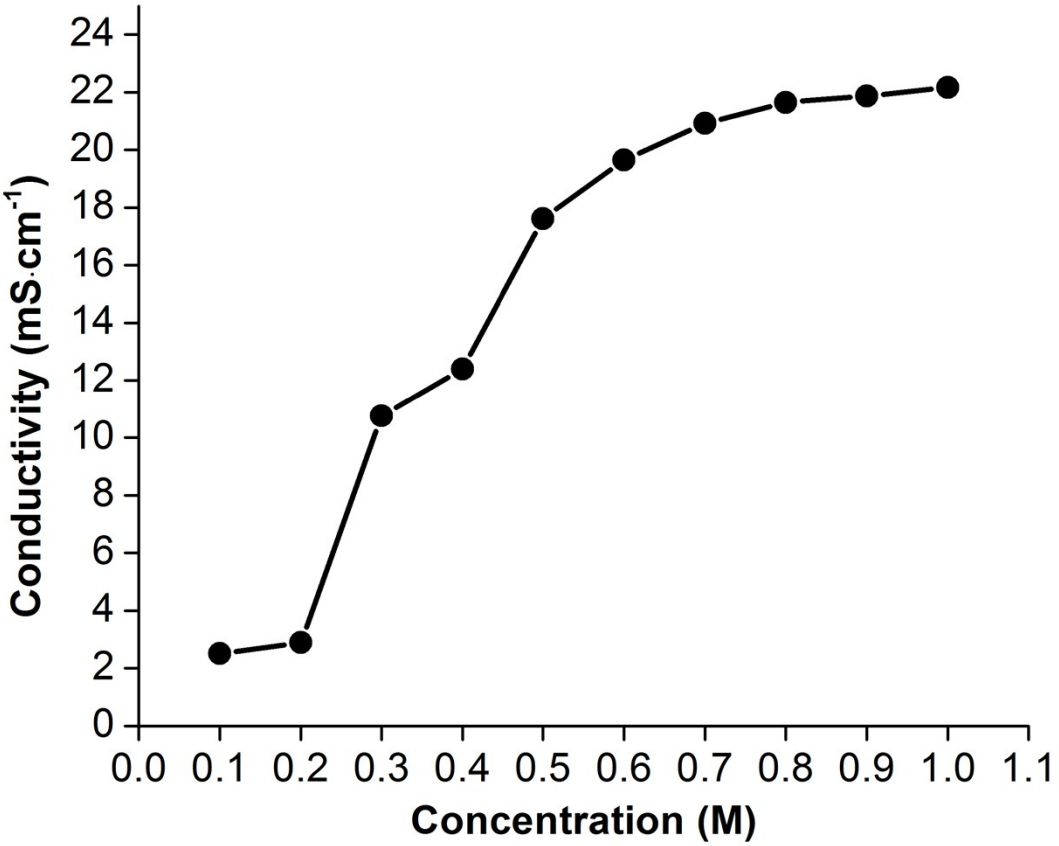

Figure S10. Room temperature conductivity of **1**[$MgPh^{1+}$] in DME as function of salt concentration.

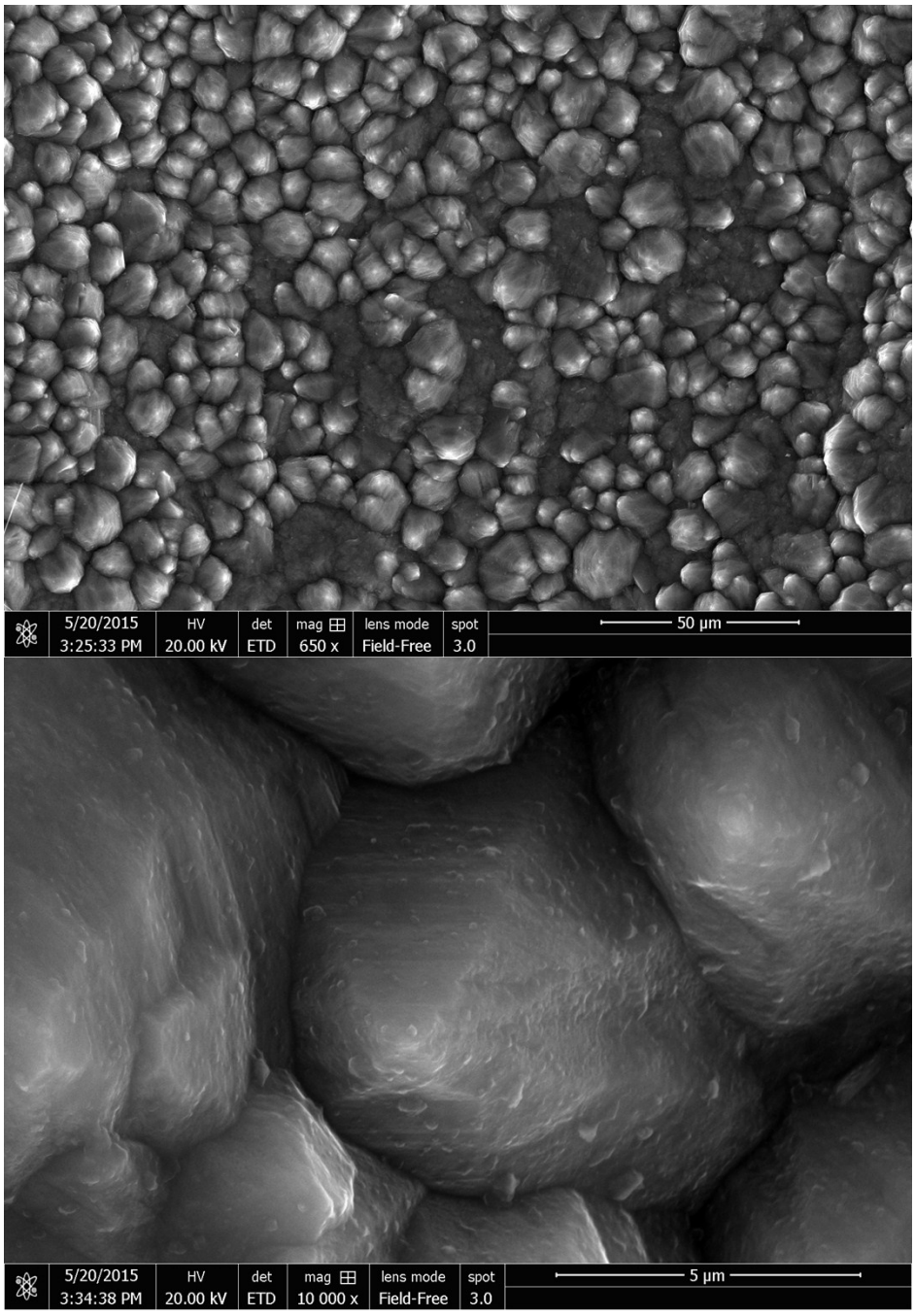

Figure S11. Scanning electron microscopy (SEM) images of Mg deposited on Pt working electrode galvanostatically with a 0.5 mA cm^{-2} current density. SEM was performed with a Nova NanoSEM 450.

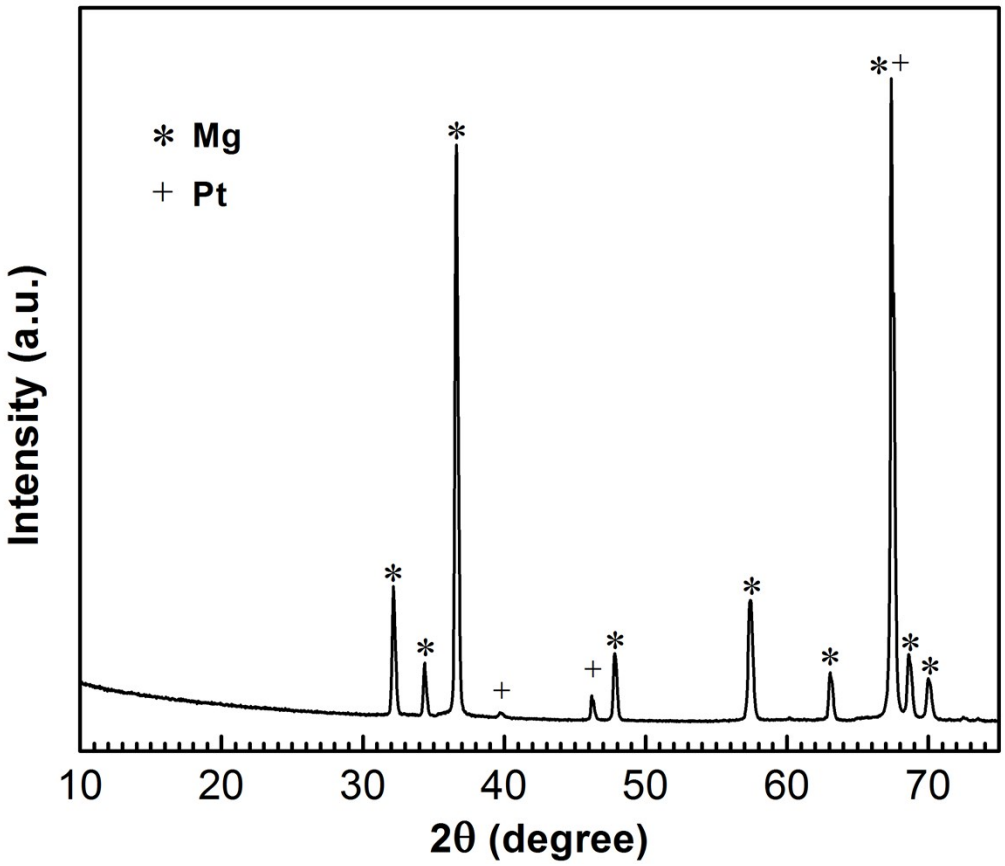

Figure S12. The X-ray diffraction (XRD) pattern of Mg deposited on Pt working electrode. The XRD was conducted using PANalytical EMPYREAN instrument (45 kV/40 mA) with a Cu-Kα source.

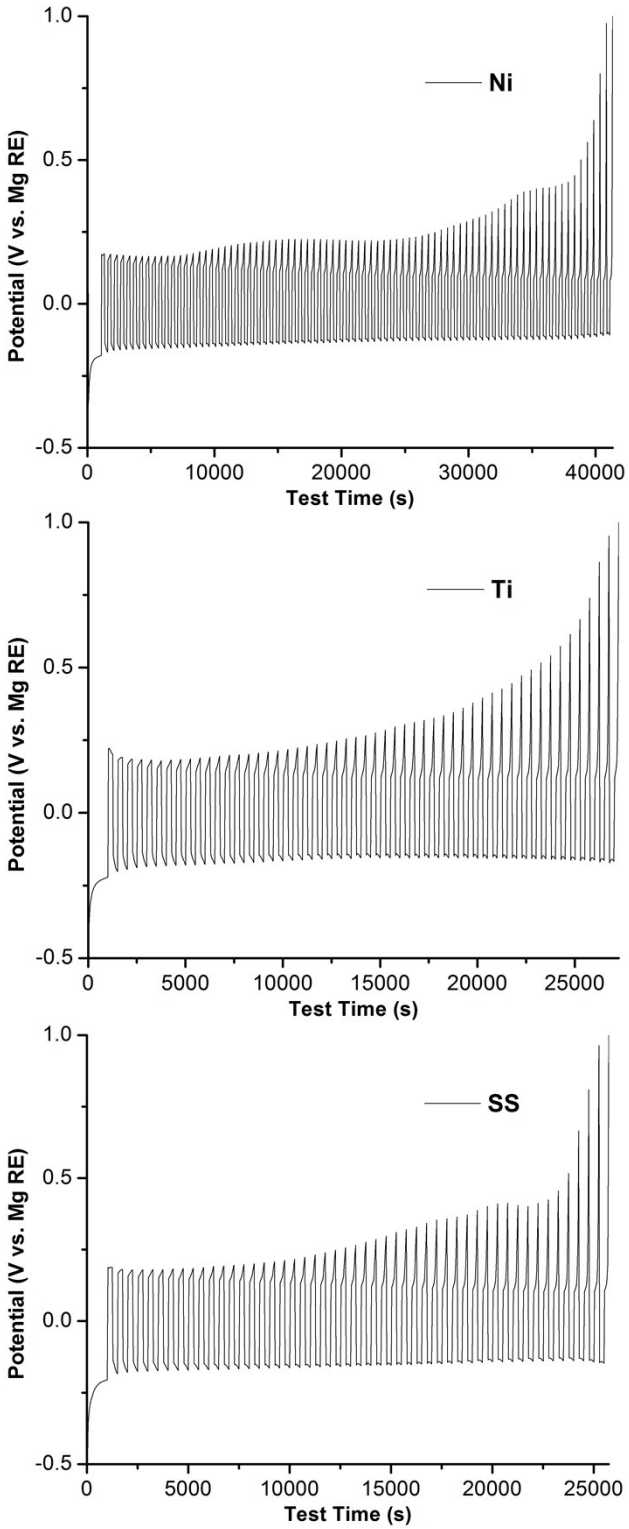

Figure S13. Galvanostatic cycling for average coulombic efficiency measurement on Ni, Ti, and SS. The ACE for Ni, Ti, and SS are 95.3%, 93.7% and 91.7%, respectively.

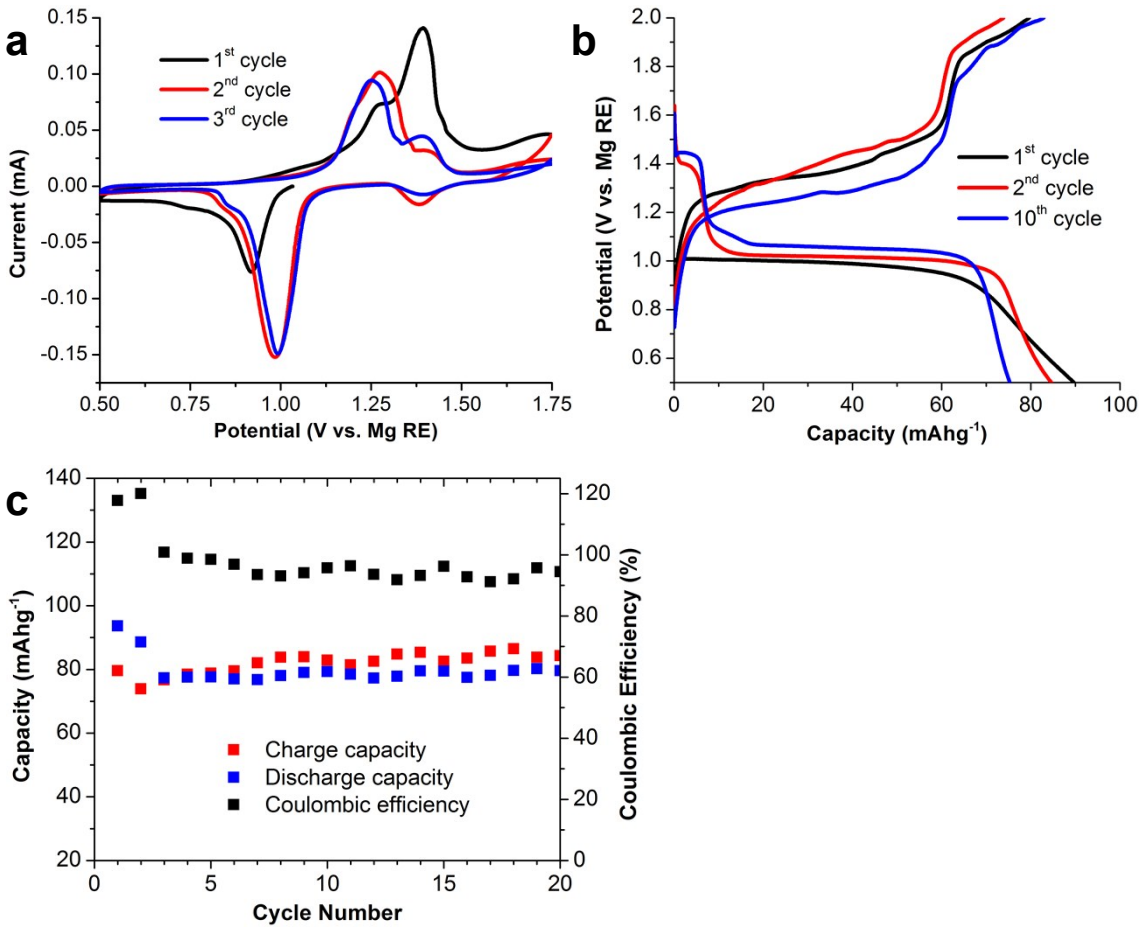

Figure S14. (a) CV (0.1 mV s^{-1} scan rate), (b) selected galvanostatic charge-discharge curves (0.1C), and (c) cycle stability (0.1C) of Mg battery with Mo_6S_8 cathode.

Reference:

[1]. C. G. Screttas, M. Micha-Screttas, *Journal of Organometallic Chemistry* **1985**, *292*, 325-333.

[2]. ***APEX 2,*** version 2014.1.1, Bruker (2014), Bruker AXS Inc., Madison, Wisconsin, USA.

[3]. ***CELL_NOW***, version 2008/4, Bruker (2012), Bruker AXS Inc., Madison, Wisconsin, USA.

[4]. ***SAINT,*** version V8.34A, Bruker (2012), Bruker AXS Inc., Madison, Wisconsin, USA.

[5]. ***TWINABS***, version 2012/1, Bruker (2012), Bruker AXS Inc., Madison, Wisconsin, USA.

[6]. ***SHELXTL,*** version 2013/4, Bruker (2013), Bruker AXS Inc., Madison, Wisconsin, USA.

[7]. P. C. Howlett, D. R. MacFarlane, and A. F. Hollennkamp, *Electrochemical and Solid-State Letters* **2004**, *7*, A97-A101.